Continuous hyperspectral absorption measurements of colored dissolved organic material in aquatic systems

Gary J. Kirkpatrick, Cristina Orrico, Mark A. Moline, Matthew Oliver, and Oscar M. Schofield

The majority of organic carbon in the oceans is present as dissolved organic matter (DOM); therefore understanding the distribution and dynamics of DOM is central to understanding global carbon cycles. Describing the time–space variability in colored dissolved organic matter (CDOM) has been difficult, as standard spectrophotometric methods for CDOM determination are laborious and susceptible to methodological biases. Previously, measurements of CDOM absorption in discrete water samples by use of a liquid-waveguide capillary cell (LWCC) compared favorably with measurements made with a benchtop spectrophotometer. Given this, we focused on automating the LWCC technique to improve our spatial and temporal sampling capabilities for CDOM. We found strong correlations between CDOM absorption spectra collected from discrete water samples using standard methods and selected corresponding CDOM spectra collected by the automated LWCC system. The near-continuous measurements by the LWCC system made it possible to map the temporal, spatial, and spectral variability of CDOM absorption along the ship track.

OCIS codes: 010.0010, 010.4450, 120.0120, 120.6200, 300.6550, 230.7370.

1. Introduction

The majority of organic carbon in the oceans is present as dissolved organic matter (DOM) and therefore understanding the distribution and dynamics of DOM is central to understanding global carbon cycles. Oceanic DOM is a heterogeneous pool of material principally consisting of degradation products of plant material often referred to as humic substances with average ages of up to 6000 years. These humic substances are composed of aromatic rings joined by long-chain alkyl structures and fall into two classes, humic acid and fulvic acid. The concentration and composition of the oceanic DOM is constantly changing because of bacterial heterotrophy and photochemical oxidation.[1–4] A significant proportion of the DOM is colored (CDOM) and is often present in concentrations sufficient to effect the color of lakes, estuaries, and near-shore coastal waters. The spectral absorption of CDOM dominates in the blue wavelengths of light as it represents an exponential curve. The exponential absorption has been described by Kalle,[5] Bricaud *et al.*,[6] and Green and Blough[7] as

$$a_{\mathrm{CDOM}}(\lambda) = a_{\mathrm{CDOM}}(\lambda_{440\,\mathrm{nm}})\exp[-S(\lambda - \lambda_{440\,\mathrm{nm}})], \quad (1)$$

where the exponential S parameter (nm^{-1}) is dependent on the composition of the CDOM present and can vary over 40%. Values of S in marine systems range from 0.011 to 0.022[8,9] whereas many freshwater systems, estuaries, and enclosed oceans exhibit even greater variability.[10,11] The humic acids, with their higher mass-specific absorption coefficients, are lost more rapidly upon entering marine waters from rivers than are the fulvic acids. This results in shifts of the slope of the CDOM absorption spectra. Hence the shape of the CDOM absorption spectra are dependent on the age of the CDOM and distance from the river source. In coastal waters, CDOM often represents the dominant optical signal, and its concentration to first order varies with the proximity to shore as terrestrial inputs represent the dominant source of CDOM. In bays near the mouths of rivers, where CDOM loading is high, the water is often referred to as black water. Water color in the coastal zone can vary rapidly in both space and time reflecting the mixing between blue ocean water and dark

G. J. Kirkpatrick (gkirkpat@mote.org) is with Mote Marine Laboratory, 1600 Ken Thompson Parkway, Sarasota, Florida 34236. C. Orrico and M. A. Moline are with the Department of Biological Sciences, California Polytechnic State University, San Luis Obispo, California 93407. M. Oliver and O. M. Schofield are with the Coastal Ocean Observation Laboratory, Institute of Marine and Coastal Sciences, 71 Dudley Road, Rutgers University, New Brunswick, New Jersey 08903.

Received 10 March 2003; revised manuscript received 8 August 2003.

0003-6935/03/336564-05$15.00/0

CDOM-ladened water. In the open ocean, far from land, there often is little CDOM signal as the only source reflects exudation from biological organisms.

Historically, describing the time–space variability in CDOM variability has been difficult as standard spectrophotometric methods used to determine the concentration of CDOM are laborious and susceptible to methodological biases. The collection and storage of discrete water samples for analysis in the laboratory often introduce artifacts such as contamination and photolysis if the sampling equipment is not properly prepared and samples are not quickly frozen. Filtration methods that are used to remove absorbing particles are somewhat subjective and can be effected by the type of filter used. Finally, frozen water samples returned to the laboratory for spectrophotometric analysis must be warmed to the same temperature as the reference water or significant error will be introduced. Overall, these many steps limit the number of samples that can be collected and effectively analyzed.

Use of the liquid waveguide capillary cell (LWCC) for CDOM absorption measurements was described by D'Sa *et al.*[12] LWCCs are made of fused-silica tubing (approximately 0.5-mm inner diameter) coated by an outer polymer layer with a refractive index lower than water. Light is introduced by an optical fiber into one end of the waveguide filled with sample water. The light is maintained in the liquid core by total internal reflection because of the higher refractive index of water relative to the polymer layer. Transmitted light exiting at the end of the liquid core is conveyed by optical fiber to a detector. The capillary waveguide can range in length from a few centimeters to several meters. The ability to form long flow cells imparts a high sensitivity to the optical system. Another advantage of the capillary waveguide over conventional absorbance cells and flow cell arrangements is the small sample volumes (a few hundred microliters) needed to fill the cell. Sample water can be introduced into the capillary cell in a number of ways including discrete injections or continuous flow.

The comparisons by D'Sa *et al.*[12] of CDOM absorption measurements of discrete water samples from two different regions using the LWCC and a benchtop spectrophotometer were favorable. Except for a slight offset of the absorption spectra obtained from the LWCC when the salinity (index of refraction) of the sample and the reference differed, the spectra from the two techniques were highly correlated. Given this outcome, we focused on automating the LWCC technique to improve our spatial and temporal sampling capabilities for CDOM. Secondarily, automating the approach minimizes the error associated with imperfect sampling, storage, and analysis on discrete samples.

A real-time automated system based on the LWCC was tested during an intensive summer field study at the Rutgers University Long-term Ecosystem Observatory (LEO-15) during a series of coastal predictive skill experiments sponsored by the U.S. Office of Naval Research. In this paper we illustrate the advantages of greatly increased spatial and temporal sampling coverage that the new approach has over the standard, discrete sample method.

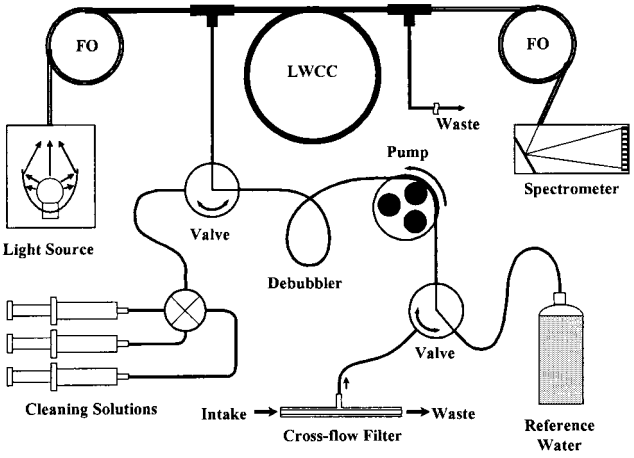

Fig. 1. Configuration of the CDOM mapper. FO, fiber-optic cable.

2. Materials and Methods

During the summer field study at the Rutgers University Long-term Ecosystem Observatory study site, the LWCC CDOM mapping system was installed on the Research Vessel *Walford* with water that was continuously pumped onboard. The CDOM mapper was run on six separate cruises between 13 and 24 July 2000. Concurrently, discrete water samples were collected, filtered, and stored at regular sampling stations for laboratory analysis of CDOM absorption at the Rutgers Marine Field Station.

The primary components of the CDOM mapper are illustrated in Fig. 1. These components included a LWCC (World Precision Instruments, Inc.) coupled to a fiber-optic spectrometer (S2000, Ocean Optics, Inc.) and a fiber-optic xenon flash lamp (PS-2, Ocean Optics, Inc.). The fiber-optic spectrometer had a spectral range from 350 to 1000 nm, a pixel resolution of 0.32 nm, and an optical resolution of approximately 1.3 nm. The spectrometer was interfaced to a notebook computer through a analog-to-digital converter (DAQCard-700, National Instruments, Inc.). Water was pumped by a miniature peristaltic pump (P625, Instech Laboratories, Inc.) through size-fractionation and cross-flow filters (MicroKros, Spectrum Laboratories, Inc.) and then through the LWCC for optical-density spectra measurements. Pure (18.2-MΩ/cm) reference water, obtained from a NANOpure (Barnstead, Inc.) water purifier, was contained in an acid-washed brown polyethylene bottle. Cleaning solutions, including pure water, hydrochloric acid, and acetone, were contained in spring-loaded 60-ml syringes connected to the LWCC with a three-way valve. Position information was obtained directly from a dedicated global positioning system (GPSMAP 135, Garmin Inc.) interfaced to the serial communication port of the notebook computer.

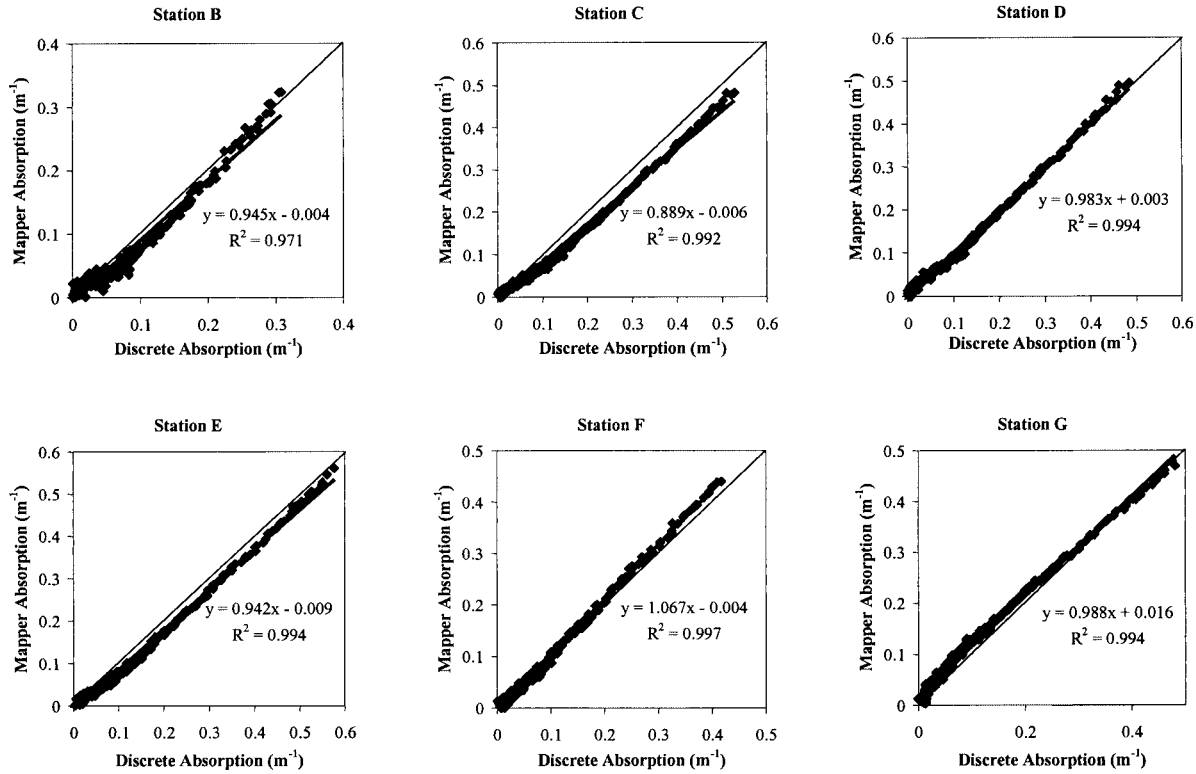

Fig. 2. Comparison between CDOM absorption spectra measured by the CDOM mapper (ordinate) and by the benchtop spectrophotometer (abscissa) on 21 July 2000. The wavelength range depicted in these plots extends from 380 to 750 nm. The heavy solid curves are a linear regression fit to the comparison with the regression equation and the correlation coefficient shown in each panel. The light solid curves are reference curves with a slope of 1.0. Figure 3 illustrates the positions of the sampling stations represented in this figure.

A continuous underway water supply was provided by tapping the flow of the ship's fire suppression system. The water intake for this system was approximately 0.5 m below the water line. Although it was not feasible to determine precisely the depth of the source water while under way, as this vessel was a displacement hull design, it was assumed that the water originated from an approximate 0.5-m depth. A primary concern in the design of the water flow and filtration scheme was to minimize the latency time between water intake and passage through the LWCC and still maintain effective filtration. A high rate of flow was maintained through the fire system. A garden hose was tapped into the fire suppression hose to bring a flow of water past the CDOM mapper in the wet laboratory. The garden hose emptied overboard and maintained a flow rate of approximately 20 l/min. A length of 9-mm Tygon tubing tapped off of the garden hose and ran to a 47-mm-diameter in-line filter holder containing a 200-mesh (74-μm opening) stainless-steel screen to provide prefiltration. The main flow of water to this filter was directed out the air vent to maintain rapid flushing of the inlet side of the filter housing. The filtrate from the in-line filter screen was carried through 3-mm Tygon tubing to a T fitting where the water flow was tapped to enter the cross-flow filter in the CDOM mapper. The majority of the filtrate from the in-line filter screen went to waste. This arrangement kept the filtrate side of the prefilter screen well flushed without having to filter the entire water stream from the ship's water system.

Because of the difference in salinity (and index of refraction) between the seawater sample and the freshwater reference, there was a slight offset of the absorption spectra collected by the CDOM mapper.[7,12] We removed this offset from each spectrum by subtracting the average value of absorption between 690 and 700 nm from each value of absorption in the spectrum. We determined the values of $a_{\mathrm{CDOM}}(440)$ and the slope S for each absorption spectrum by fitting Eq. (1) using the least-squares method. We created contour maps of $a_{\mathrm{CDOM}}(440)$ with Surfer (Golden Software, Inc.) utilizing data collected by the CDOM mapper.

Discrete water samples were collected from the surface by a Niskin bottle at selected stations along the ship track. Hence the discrete samples integrated approximately 0.5 m of the near-surface water column, approximating the collection zone of the flow-through system (fire suppression system). The water was filtered by low vacuum (<8-cm Hg) through 0.2-μm membrane filters. The filtrate was frozen in brown polyethylene bottles. We conducted the absorbance measurements in the laboratory within 12 h using a Shimadzu Model 2501 UV–visible scanning benchtop spectrophotometer with a 10-cm path-length cell and NANOpure water as the refer-

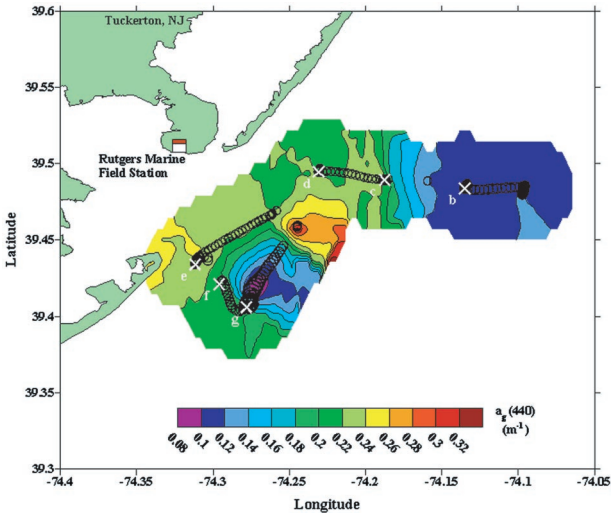

Fig. 3. Contour map of CDOM absorption at 440 nm produced from CDOM mapper data for 21 July 2000. Open circles indicate the central position where the CDOM mapper determined average CDOM absorption spectra. The size of the circle represents the value of S, the slope of the CDOM spectrum at 440 nm, which ranged from 0.017 to 0.026 nm^{-1}. Lettered crosses indicate sampling stations where discrete water samples were collected for CDOM absorption determinations on a benchtop spectrophotometer.

ence. The spectrophotometer scan range was set to 300–750 nm with 1-nm scan resolution and 2-nm spectral bandwidth.

3. Results

Discrete water samples for analysis in a benchtop spectrophotometer were collected on five of the six days that spectra were obtained by the CDOM mapper. The operating sequence of the CDOM mapper included periods of time when sample spectra were not collected for periods of up to 15 min while the waveguides were automatically cleaned, and new dark current and reference spectra were collected. These gaps in the sample spectra occasionally occurred when discrete water samples were collected, limiting the number of times when both methods were conducted simultaneously. On 21 July 2000 six discrete spectra were collected that coincided in time with spectra collected by the CDOM mapper (Fig. 2). The average slope of linear regressions of these six pairs of spectra was 0.97 ± 0.06, and the average correlation coefficient was 0.99. A slight wavelength-dependent difference was seen in the comparison of the two methods. The difference peaked at approximately 500 nm and always resulted from the CDOM mapper spectra having a higher slope than the spectrophotometer spectra. There were no apparent spatially related trends in the comparisons. The comparison station furthest offshore had the lowest correlation coefficient (0.97) but that may have been due to the lower absorption signal (lower signal-to-noise ratio), not to spatial trends in the measurements.

During the survey on 21 July 2000 a patch of low-

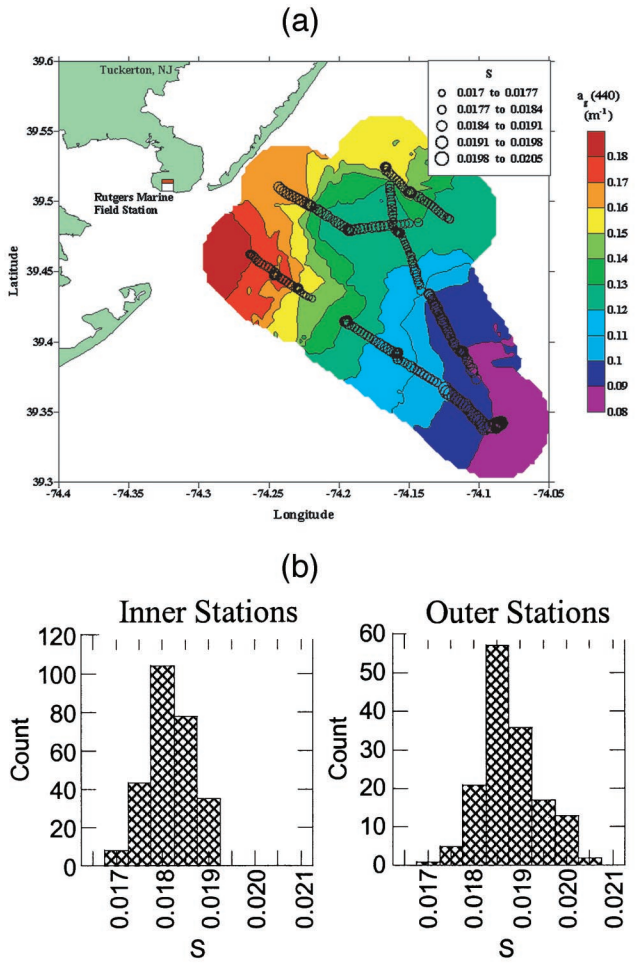

Fig. 4. (a) Contour map of CDOM absorption at 440 nm produced from CDOM mapper data for 17 July 2000. Open circles indicate the central position where the CDOM mapper determined average CDOM absorption spectra. The size of the circle represents the value of S, the slope of the CDOM spectrum at 440 nm, which ranged from 0.017 to 0.020 nm^{-1}. (b) Histograms show the distribution of S over the inner and outer sample stations.

CDOM water had intruded well inshore (Fig. 3) relative to the distribution seen on 17 July 2000 (Fig. 4). The distribution of CDOM absorption on 17 July 2001 illustrates the typical strong gradient from high values near sources of terrestrial input to low values in offshore waters that are influenced by clean oceanic water. Figures 3 and 4 also illustrate the variability of S in coastal waters. Values of S obtained during the two days reported here ranged from 0.008 to 0.026. Generally, the lower values were observed near the shores associated with higher concentrations of CDOM. This indicates that the near-shore waters contained more recently produced CDOM. Because coastal CDOM is terrestrially derived, the closer the water is to the source (land) the higher is the CDOM content. In addition, fresher CDOM has had less time to be acted upon by sunlight, which causes photolysis, a process that removes the more labile compounds, leaving the more refractory compounds. The labile compounds exhibit absorption

spectra with shallower slopes than do refractory compounds.

4. Discussion

Recent literature has raised a concern that the quartz liquid waveguide is subject to unpredictable variability when applied to seawater analysis.[13] This concern was alleviated by D'Sa and Steward[14] and by the results of the research reported here. These results clearly show that, correcting for the difference in refractive index between the seawater sample and the freshwater reference, we obtain results with the quartz capillary waveguide that are comparable to the standard methods with benchtop spectrophotometers. Furthermore, interference by bubbles trapped in the capillary waveguide is a constant concern with capillary waveguides, and the quartz waveguide has been slightly more forgiving about bubble formation and persistence than has the amorphous Teflon waveguide proffered by Byrne and Kaltenbacher.[13] Finally the configuration of the CDOM mapper has most recently been changed to incorporate two waveguides that can operate on an alternating schedule. This has helped to reduce the gaps in the data record caused by cleaning and new reference spectrum collection. Additional field trials are required to verify the applicability of this approach to water types ranging from estuarine to oceanic.

There was an excellent quantitative agreement between the absorption spectra collected by the CDOM mapper and the spectra measured by a benchtop spectrophotometer on discrete water samples. Some of the variability between the two measurement approaches can be attributed to the different sample collection methods (flow-through versus Niskin bottle) in the near-surface water column where strong gradients could have been present. The good correlation between these spectra collected by the two methods suggests that the CDOM mapper provided accurate maps allowing the ship to resolve the time, space, and spectral variability in the CDOM absorption. The dramatic variability in the CDOM absorption clearly illustrated the high degree of variability present in these coastal waters that could not have been resolved by traditional discrete CDOM sampling techniques. High-resolution maps such as this will dramatically improve our ability to ground truth the CDOM maps that are currently estimated by ocean color satellite imagery.

The feasibility of collecting hyperspectral data will allow for the first time to our knowledge the comprehensive mapping of the exponential slope S factor. The variability in the S value reflects the composition of the material present within the CDOM pool. Given this, maps may provide a means to develop an empirical, but quantitative, understanding of factors associated with specific S values. This would allow a set of environmental paradigms to be tested by means of relating variability in the S value to autotrophic particulate carbon, total organic carbon, primary productivity, and nutrient fluxes. This will be especially important for coastal water quality managers where CDOM cycling is greatest reflecting higher levels of primary production (which yield larger quantities of total DOM) and CDOM loading from terrestrial runoff.

The CDOM mapper has recently been reduced in size to fit in three types of autonomous underwater vehicle. These include buoyancy-driven underwater gliders, vertical profilers and propeller-driven surveyors. In addition, deployments on fixed platforms (moorings and pilings) are under way in coastal and estuarine waters. With these deployment options it will be possible to provide comprehensive three-dimensional views of CDOM absorption characteristics for the developing ocean observatory network.

References

1. P. M. Williams and E. R. M. Druffel, "Radiocarbon in dissolved organic matter in the central North Pacific Ocean," Nature (London) **330,** 246–248 (1987).
2. R. J. Kieber, L. H. Hydro, and P. J. Seaton, "Photooxidation of triglycerides and fatty acids in seawater: implications toward the formation of marine humic substances," Limnol. Oceanogr. **42,** 1454–1462 (1997).
3. W. L. Miller and M. A. Moran, "Interaction of photochemical and microbial processes in the degradation of refractory dissolved organic matter from a coastal marine environment," Limnol. Oceanogr. **42,** 417–420 (1997).
4. M. A. Moran and R. G. Zepp, "Role of photoreactions in the formation of biologically labile compounds from dissolved organic matter," Limnol. Oceanogr. **42,** 1307–1316 (1997).
5. K. Kalle, "The problem of the gelbstoff in the sea," Oceanogr. Mar. Biol. Ann. Rev. **4,** 91–104 (1966).
6. A. Bricaud, A. Morel, and L. Prieur, "Absorption by dissolved organic matter of the sea (yellow substance) in the UV and visible domains," Limnol. Oceanogr. **26,** 43–53 (1981).
7. S. A. Green and N. V. Blough, "Optical absorption and fluorescence properties of chromophoric dissolved organic matter in natural waters," Limnol. Oceanogr. **39,** 1903–1916 (1994).
8. K. L. Carder, R. G. Steward, G. R. Harvey, and P. B. Ortner, "Marine humic and fulvic acids: their effects on remote sensing of ocean chlorophyll," Limnol. Oceanogr. **34,** 68–81 (1989).
9. C. S. Roesler, M. J. Perry, and K. L. Carder, "Modeling *in situ* phytoplankton absorption from total absorption spectra in productive inland marine waters," Limnol Oceanogr. **34,** 1510–1523 (1989).
10. N. G. Jerlov, *Marine Optics* (Elsevier, New York, 1976).
11. J. T. O. Kirk, "Yellow substance (gelbstoff) and its contribution to the attenuation of photosynthetically active radiation in some inland and coastal southeastern Australian waters," Aust. J. Mar. Freshwater Res. **27,** 61–71 (1976).
12. E. J. D'Sa, R. G. Steward, A. Vodacek, N. V. Blough, and D. Phinney, "Determining optical absorption of colored dissolved organic matter in seawater with a liquid capillary waveguide," Limnol. Oceanogr. **44,** 1142–1148 (1999).
13. R. H. Byrne and E. Kaltenbacher, "Use of liquid core waveguides for long pathlength absorbance spectroscopy: principles and practice," Limnol. Oceanogr. **46,** 740–742 (2001).
14. E. J. D'Sa and R. G. Steward, "Liquid capillary waveguide application in absorbance spectroscopy (reply to the comment by Byrne and Kaltenbacher)," Limnol. Oceanogr. **46,** 742–745 (2001).